Self-consistent-phonon-approximation study of a double Morse hydrogen-bonded chain

O. Yanovitskii,* G. Vlastou-Tsinganos, and N. Flytzanis
Physics Department, University of Crete, Heraklion, Greece
(Received 14 June 1993)

We propose a one-dimensional hydrogen-bonded chain model, where temperature is introduced using a variational form of the self-consistent-phonon-approximation method to evlauate the semiquantum free energy. The parameters of the model are chosen self-consistently and the hydrogen bond is described by a double Morse interaction. The behavior of the chain is studied with a defect and without one and the Peierls barrier is calculated. Introduction of an anharmonic O-O interaction results in slight qualitative changes.

I. INTRODUCTION

There are many hydrogen-bond solid-state systems consisting of one-dimensional chains like imidazole,[1] acetanilide,[2] hydrogen halides[3] (HF, HCl, HBr), lithium hydrazinium sulfate[4] ($LiN_2H_5SO_4$), and proteins across biomembranes.[5] Protonic conductivity in such systems in the direction of the hydrogen-bonded chains is about 10^3 times greater than in the other two directions.[6] In fact, it can be comparable or even larger than the protonic conductivity in ice.[7] Many two- or three-dimensional systems can be regarded as a compound system of multiply linked one-dimensional H-bonded chains. This is the case with the Bernal-Fowler filaments in ice,[8] or the four helices in the polypeptide of bacteriorhodopsin in holobacterium holobium.[9] While it has not been possible to determine the exact conductivity mechanism,[10] the existence and mobility of ionic or bonding defects play a crucial role in electrical conductivity and dielectric response.[8,11–13] However, both their equilibrium concentrations and mobilities are indirectly determined quantities from the analysis of the experiments.

In what follows we shall use the example of Bernal-Fowler filaments in ice, where there is considerable experimental data. In the model to be discussed, the techniques and the qualitative conclusions are valid for various hydrogen-bonded systems, but the parameters to be used are taken for ice, where many measurements exist. In ice, the transfer of a proton from one water molecule to the next, creates a hydroxonium (H_3O^+) with a positive effective charge (about $0.62e$) and a hydroxyl (OH^-) with a negative effective one, which can migrate under an applied electric field. The activation energy for the creation of a pair of ionic defects is 0.96 eV. It is also accepted that the creation of bonding or rotational Bjerrum defects is necessary to keep pumping the conduction mechanism in a two-step relay process.[14]

For an ionic defect to move, it must overcome a considerable barrier, so that hopping-type motion cannot be effective. For this reason solitonic models of collective proton motion, which present a lower barrier seem very promising. This includes models with collective proton motion in rigid or moving substrates. In fact, the two sublattice models[15] can lower the effective barrier by contraction of the heavy-ion separation.[15] This happens for both optical-type motion about the O-O center of mass or for acoustic motion. Improvements have been introduced, where the substrate has two barriers,[17] so that it allows the simultaneous existence of ionic and Bjerrum defects.[18]

In almost all the previous work, however, temperature has not been taken into account while quantum effects were neglected. However, even at zero temperature, quantum effects for a light species in a potential with narrow wells can be very important. It is known that the Peierls barrier of dislocations in crystals can vary very strongly with the dislocation width.[19,20] Thus the activation energy for motion of the ionic defects dressed with thermal and quantum fluctuations will vary with temperature. So that over a temperature range, it is possible to have either a situation of single proton hopping for a narrow defect and correspondingly a large Peierls barrier, which does not contribute to conductivity significantly, or a ballistic-type solitonic motion.

In this paper, we will introduce temperature to study the structure of a defectless chain and the Peierls barrier of an ionic defect. This is very useful since it is a parameter that will enter in any model to explain conductivity. Temperature can be introduced using a variational form of the self-consistent phonon approximation (SCPA)[21,22] for the evaluation of the semiquantum free energy. SCPA has been used extensively in the past for light noble gas atoms, where quantum effects can be significant, and for ferroelectrics, where the dipole moments can have two equivalent orientations. This corresponds to the two degenerate minima of a double-well potential in the absence of an external field.

In Sec. II we will discuss the hydrogen-bonded chain model we study. In Sec. III we describe the SCPA variational method we used to evaluate the free energy for the chain with a defect or without one. In Sec. IV, we give values for the physical parameters used in the model, and discuss their large variability in the literature. In Sec. V, we present the numerical results, while in Sec. VI an anharmonic O-O interaction is taken into consideration. In Sec. VII, we present a discussion emphasizing the results that must be taken into consideration, when constructing a model to explain conductivity.

0163-1829/93/48(17)/12645(10)/$06.00

II. DESCRIPTION OF THE MODEL

In ice or more complex biological systems, the proton transfer takes place along the Bernal-Fowler filaments. It has been a common practice, after the work of Antonchenko, Davydov, and Zolotariuk,[23] to represent such a filament, by a one-dimensional (1D) chain consisting of two interacting sublattices. The one is made of protons (H) and the other one of the heavy ions, here to be called oxygen atoms (O). Each proton "belongs" to two oxygens and it can jump between two equivalent positions of the double-well potential along an O—O bond. The form of this potential used in the literature, may vary from a piecewise quadratic[24] to a ϕ^4 (Refs. 23 and 25) or a Morse potential,[26,27] depending on the method used. For example, the piecewise quadratic potential is convenient for analytical computations, while the ϕ^4 potential has been used in the continuum lattice limit approximation. As for the Morse potential, it is widely accepted that it is a more realistic description of the hydrogen bond.

In the present work we consider a Morse potential for the coupling between the two sublattices so that the proton feels a symmetric double Morse (DM) potential, centered between every two oxygens. Its variable is the relative position of the proton and the oxygen and has an important property (as shown in Fig. 1): the barrier between the two wells is much lower when the two neighboring oxygens approach each other. This is an essential ingredient, which allows an easier migration of the protons, when the bond is stronger.

The oxygen displacements (ρ_n) are measured from the fixed oxygen positions while the proton (u_n) displacements are measured from the middle point between equilibrium positions of the oxygen atoms. Displacements ρ_n and u_n are continuous variables that depend on the discrete lattice site n. Thus the double Morse potential part of the Hamiltonian is

$$\begin{aligned}\mathcal{H}_{\mathrm{OH}}=&\sum_n [D(1-e^{-d(R/2+u_n-\rho_n-r_e)})^2 \\ &+D(1-e^{-d(R/2-u_n+\rho_{n+1}-r_e)})^2] \\ =&\sum_n U^n_{\mathrm{OH}} \ . \end{aligned} \tag{1}$$

R is the equilibrium lattice spacing of the oxygen sublattice and the potential parameters are the potential well depth D, the position of the minima r_e measured from the oxygens, and the force constant which is related to d ($k_{\mathrm{OH}}=2d^2D$).

The protons (of mass m) are coupled to each other by a harmonic interaction depending on their relative displacements, with a characteristic force constant k_{HH}:

$$\mathcal{H}_{\mathrm{H}}=\frac{1}{2}\sum_n \left[\frac{\hbar^2}{m}\frac{\partial^2}{\partial u_n^2}+k_{\mathrm{HH}}(u_{n+1}-u_n)^2\right] . \tag{2}$$

In the last part of the Hamiltonian, the oxygens (of mass M) are subject to a parabolic on-site potential, to simulate the environment with a force constant k and a harmonic coupling, which depends on their relative position and the force constant K_{OO}

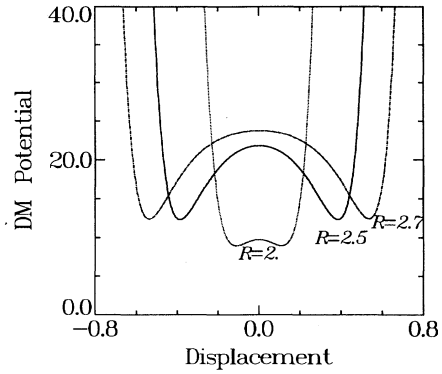

FIG. 1. The barrier of the double Morse potential increases as two oxygens are far apart and it reduces as they approach each other.

$$\mathcal{H}_{\mathrm{O}}=\frac{1}{2}\sum_n \left[-\frac{\hbar^2}{M}\frac{\partial^2}{\partial\rho_n^2}+k\rho_n^2+k_{\mathrm{OO}}(\rho_{n+1}-\rho_n)^2\right] . \tag{3}$$

The Hamiltonian of the model is the sum of the above three terms:

$$\mathcal{H}=\mathcal{H}_{\mathrm{OH}}+\mathcal{H}_{\mathrm{H}}+\mathcal{H}_{\mathrm{O}} . \tag{4}$$

III. THE VARIATIONAL METHOD

Introduction of temperature in a nonlinear system, in the exact quantum-mechanical regime is a rather impossible calculation even for the one degree of freedom for a discrete system. Therefore, one has to limit oneself to an approximation for the free energy like SCPA, which includes zero-order quantum fluctuations. The evaluation of an upper limit to the free energy is based on the Gibbs-Bogoliubov inequality:[28]

$$\mathcal{F}\le\tilde{\mathcal{F}}=\mathcal{F}_0+\langle\mathcal{H}-\mathcal{H}_0\rangle_0 . \tag{5}$$

$\mathcal{H}_0$ is a trial Hamiltonian, chosen as a variational Hamiltonian for $\mathcal{H}$, and $\mathcal{F}_0$ is its respective free energy. Quantum mechanics enter in the calculation of $\mathcal{F}_0$ and the expectation value $\langle\cdots\rangle$, which is evaluated by the quantum density matrix of $\mathcal{H}_0$. The choice of $\mathcal{H}_0$ is practically limited by the fact that its $\mathcal{F}_0$ and density matrix δ_0 must be known exactly. Therefore, we use a set of independent displaced harmonic oscillators[29] for each lattice site, that is a self-consistent phonon approach:[30]

$$\begin{aligned}\mathcal{H}_0=\frac{1}{2}\sum_n \Bigg[&-\frac{\hbar^2}{m}\frac{\partial^2}{\partial u_n^2}+m\omega_{H,n}^2(u_n-\alpha_{H,n})^2 \\ &+\frac{\hbar^2}{M}\frac{\partial^2}{\partial\rho_n^2}+M\omega_{\mathrm{O},n}^2(\rho_n-\alpha_{\mathrm{O},n})^2\Bigg] .\end{aligned} \tag{6}$$

This independent-site approximation is improved by choosing different parameters at each site, for each type of atom: the local oscillator frequency and its mean position. The free energy corresponding to $\mathcal{H}_0$ is well known analytically:

$$\mathcal{F}_0=\sum_n \left[\frac{\hbar\omega_{\mathrm{H},n}}{2}+k_BT\ln(1-e^{-\hbar\omega_{\mathrm{H},n}/k_BT}) + \frac{\hbar\omega_{\mathrm{O},n}}{2}+k_BT\ln(1-e^{-\hbar\omega_{\mathrm{O},n}/k_BT}) \right] . \quad (7)$$

These parameters α and ω, are used now variationally in order to minimize the free energy $\tilde{\mathcal{F}}$. The density matrix for one harmonic oscillator,

$$\delta_0(y,y)=\left[\frac{m\omega}{2\pi\sinh(\hbar\omega/k_BT)} \right]^{1/2} \times\exp\left[-\frac{m\omega}{\hbar}\tanh\left[\frac{\hbar\omega}{2k_BT} \right] y^2 \right] \quad (8)$$

is incorporated in the calculation of the expectation value of Eq. (5), which permits analytic evaluation of the integrals. Therefore,

$$\langle \mathcal{H}-\mathcal{H}_0\rangle_0=\sum_n \left[\frac{1}{2}k_{\mathrm{HH}}\left[\frac{1}{\gamma_{\mathrm{H},n}}+(\alpha_{\mathrm{H},n}-\alpha_{\mathrm{H},n+1})^2 \right]+\frac{1}{2}k_{\mathrm{OO}}\left[\frac{1}{\gamma_{\mathrm{O},n}}+(\alpha_{\mathrm{O},n}-\alpha_{\mathrm{O},n+1})^2 \right] + \frac{1}{2}k\left[\frac{1}{2\gamma_{\mathrm{O},n}}+\alpha_{\mathrm{O},n}^2 \right]-\frac{m}{4}\frac{\omega_{\mathrm{H},n}^2}{\gamma_{\mathrm{H},n}}-\frac{M}{4}\frac{\omega_{\mathrm{O},n}^2}{\gamma_{\mathrm{O},n}}+\langle U_{\mathrm{OH}}^n\rangle \right] , \quad (9)$$

and

$$\begin{aligned}\langle U_{\mathrm{OH}}^n\rangle = D\Bigg\{ & 2-2\exp\left[\frac{d^2}{4}\left[\frac{1}{\gamma_{\mathrm{H},n}}+\frac{1}{\gamma_{\mathrm{O},n}} \right]-d\left[\frac{R}{2}+\alpha_{\mathrm{H},n}-\alpha_{\mathrm{O},n}-r_e \right] \right] \\ & +\exp\left[d^2\left[\frac{1}{\gamma_{\mathrm{H},n}}+\frac{1}{\gamma_{\mathrm{O},n}} \right]-2d\left[\frac{R}{2}+\alpha_{\mathrm{H},n}-\alpha_{\mathrm{O},n}-r_e \right] \right] \\ & -2\exp\left[\frac{d^2}{4}\left[\frac{1}{\gamma_{\mathrm{H},n}}+\frac{1}{\gamma_{\mathrm{O},n+1}} \right]-d\left[\frac{R}{2}-\alpha_{\mathrm{H},n}+\alpha_{\mathrm{O},n+1}-r_e \right] \right] \\ & +\exp\left[d^2\left[\frac{1}{\gamma_{\mathrm{H},n}}+\frac{1}{\gamma_{\mathrm{O},n+1}} \right]-2d\left[\frac{R}{2}-\alpha_{\mathrm{H},n}+\alpha_{\mathrm{O},n+1}-r_e \right] \right] \Bigg\} , \end{aligned} \quad (10)$$

where

$$\gamma_{\mathrm{H},n}=\frac{m\omega_{\mathrm{H},n}}{\hbar}\tanh\left[\frac{\hbar\omega_{\mathrm{H},n}}{2k_BT} \right] , \quad (11)$$

$$\gamma_{\mathrm{O},n}=\frac{M\omega_{\mathrm{O},n}}{\hbar}\tanh\left[\frac{\hbar\omega_{\mathrm{O},n}}{2k_BT} \right] . \quad (12)$$

The approximate free energy $\tilde{\mathcal{F}}$ now is a function of the variational parameters $\alpha_{\mathrm{H},n}$, $\alpha_{\mathrm{O},n}$, $\omega_{\mathrm{H},n}$, and $\omega_{\mathrm{O},n}$, that are actually the mean particle displacement and the local frequency. For the numerical minimization we use both the simulated annealing Monte Carlo (SAMC) method[31,32] and the gradient method. The SAMC method was used selectively to check for the global minimum where it is very efficient. Additionally, the steepest descent or another gradient method is helpful to locate the exact minimum while already in the potential well minimum. In Ref. 33, the ground state of the system was investigated using the SAMC method and it was found that the assumed period 1 structure is the ground state. Thus in this work we use the gradient method since the global minimum is already known.

IV. PARAMETERS OF THE MODEL

It is a common practice (Ref. 34 and references therein) to model the proton transport in quasi-one-dimensional hydrogen-bonded systems, with a 1D ice crystal. The way, though, that the physical parameters of the DM symmetrical potential describing the O—H · · · O hydrogen bond are chosen, is quite different.[35,26,27] Table I shows several sets of the DM potential parameters taken from different sources. The big variety in these sets of parameters reflects the different approaches used to fit them. Kryachko[26] defines the DM parameters from *ab initio* calculations of the $(H_5O_2)^+$ complex. In Ref. 27 the rather different parameters come from experimental values of the barrier height in the double-well potential and also from spectroscopic characteristics of the H bonds in ice. The set of the DM parameters from the Matsushita and Matsubara paper[35] is the result of analysis of geometric and spectroscopic characteristics of the O—H · · · O bonds. Finally, *ab initio* cal-

TABLE I. Parameters of double Morse potential.

D (kcal/mole)	d (Å^{-1})	r_e (Å)	Reference number
69.98	2.77	0.97	26
9.27	7.39	1.01	27
50.00	2.89	0.95	35
76.04	2.68	0.97	39

TABLE II. Set of parameters used in the numerical simulations.

D (kcal/mole)	d (Å^{-1})	r_e (Å)	R (Å)	k_{OO} (N/m)	k (N/m)	k_{HH} (N/m)
10.7	7.8	0.94	2.76	36.6	29.1	22.0

culations of the parameters of the DM potential are given in a very recent paper.[38] The authors here fitted the proton transfer potentials in protonated water and ammonia pentamers by several simple analytical functions such as ϕ^4, Gaussian, sinusoidal, Morse function, and fourth-order polynomial. The Morse potential gives the best results and, most importantly, it is found to be fairly insensitive to the H-bond length, i.e., the same parameters in the Morse potential can fit the energy profile for proton movement for various O-O distances.

The DM potential depends on four parameters that have to be defined: the equilibrium distance between oxygens R, the potential well depth D, the O-H equilibrium length of the single Morse potential r_e, and the exponential factor d related to the harmonic force constant of the O—H bond. Our choice of $R=2.76$ Å is the well known value of the O-O distance in ice *Ih*. In order to define the parameters D, d, and r_e we use the following characteristic values of ice *Ih*: the critical distance of disappearance of the double well $R_{cr}=2.38$ Å,[26] the O-H bond length $r_0=1.01$ Å,[36] and the force constants $K_{OH}=658$ N/m, $k_{OO}=36.6$ N/m and $k=29.1$ N/m.[37] The ion mass is $M=17m=17m_p$, where m_p is the proton mass, and the hydrogen-hydrogen coupling constant is taken as $k_{HH}=22$ N/m.[27] It should be mentioned here that the value of this constant is not uniquely experimentally known and therefore it has been calculated theoretically in a number of ways. A detailed analysis of the H-H coupling in H-bonded chains based on *ab initio* calculations of water and ammonia pentamers is performed by Duan and Scheiner.[39] The value of the hydrogen-hydrogen coupling force constant defined there is close to the one used in the present paper. The calculation of the parameters of the DM potential should take into account the change of the potential relief due to quantum and temperature effect. In the framework of the SCPA approach proposed here, the DM part of the potential is given by Eq. (10). The self-consistent method for the calculation of the parameters D, d, and r_e is presented in the Appendix. The results of this calculation are shown in Table II.

V. RESULTS OF THE NUMERICAL CALCULATIONS

A. Ground state

In order to be able to study the structure and energies of the ionic defects in the present hydrogen-bonded chain model, we must define the ground state of the unperturbed system. Using the SAMC method it was verified that the period 1 structure is indeed the ground state for the system in the range of parameters used.[33] Here we use a simple analytical approach to treat period 1 structure and one can obtain simple expressions for the variational parameters that is due to the use of the DM potential.

First of all we have to minimize the free energy $\tilde{\mathcal{F}}$ for the chain with a structure of period equal to one lattice spacing R. In that case, we have the following conditions for the variational parameters:

$$\omega_{H,n}=\omega_H,\quad \omega_{O,n}=\omega_O,\quad \alpha_{H,n}=\alpha_H\ ,$$
$$\alpha_{O,n}=\alpha_O \text{ for all } n\ . \tag{13}$$

These conditions describe an unperturbed chain, where all protons and oxygens occupy correspondingly equivalent positions. Using the free energy $\tilde{\mathcal{F}}$ expressions shown in Eqs. (5), (7), (9), and (10), and taking into account the conditions (13), we have

$$0=\frac{\partial\tilde{\mathcal{F}}}{\partial\alpha_H}=\frac{\partial\langle U_{OH}\rangle}{\partial\alpha_H}\ , \tag{14}$$

$$0=\frac{\partial\tilde{\mathcal{F}}}{\partial\alpha_O}=k\alpha_O+\frac{\partial\langle U_{OH}\rangle}{\partial\alpha_O}\ , \tag{15}$$

$$0=\frac{\partial\tilde{\mathcal{F}}}{\partial\omega_H}=\left[\frac{k_{HH}}{2}-\frac{m\omega_H^2}{4}+\frac{\partial\langle U_{OH}\rangle}{\partial(1/\gamma_H)}\right]\frac{d}{d\omega_H}\left[\frac{1}{\gamma_H}\right],$$
$$0=\frac{\partial\tilde{\mathcal{F}}}{\partial\omega_O} \tag{16}$$
$$=\left[\frac{k_{OO}}{2}+\frac{k}{4}-\frac{m\omega_O^2}{4}+\frac{\partial\langle U_{OH}\rangle}{\partial(1/\gamma_O)}\right]\frac{d}{d\omega_H}\left[\frac{1}{\gamma_O}\right], \tag{17}$$

where

$$\gamma_H=\gamma_{H,n}|_{\omega_{H,n}=\omega_H}\ , \tag{18}$$

$$\gamma_O=\gamma_{O,n}|_{\omega_{O,n}=\omega_O}\ . \tag{19}$$

Noting that

$$\frac{\partial\langle U_{OH}\rangle}{\partial\alpha_O}=-\frac{\partial\langle U_{OH}\rangle}{\partial\alpha_H}\ ,$$

we obtain the following solutions of Eqs. (14)–(15):

$$\alpha_O=0\ , \tag{20}$$

and three possible solutions for α_H with

$$\alpha_H^{(0)}=0 \tag{21}$$

or

$$\alpha_H^{(1,2)}=\pm\frac{1}{d}\operatorname{arcosh}\left\{\frac{1}{2}\exp\left[-\frac{3}{4}d^2f+d\left[\frac{R}{2}-r_e\right]\right]\right\}, \tag{22}$$

where

$$f=\frac{1}{\gamma_H}+\frac{1}{\gamma_O}\ . \tag{23}$$

Using

$$\frac{\partial\langle U_{OH}\rangle}{\partial(1/\gamma_H)}=\frac{\partial\langle U_{OH}\rangle}{\partial(1/\gamma_O)}\ ,$$

from Eqs. (16) and (17) we have for ω_O and ω_H the following equations:

$$k_{HH}-\frac{m\omega_H^2}{2}=k_{OO}+\frac{k}{2}-\frac{M\omega_O^2}{2}\ , \tag{24}$$

$$\omega_H^2=\frac{1}{m}\left[2k_{HH}+4\frac{\partial\langle U_{OH}\rangle}{\partial(1/\gamma_H)}\right]\ . \tag{25}$$

Substituting (21) in (25), we obtain

$$\omega_{H,0}^2=\frac{2}{m}[k_{HH}+2Dd^2(-e^{d^2f/4-d(R/2-r_e)}+2e^{d^2f-2d(R/2-r_e)})]\ . \tag{26}$$

Analogously, from (22) and (25) we have

$$\omega_{H,1,2}^2=\frac{2}{m}[k_{HH}+Dd^2(e^{-d^2f/2}-4e^{d^2f-2d(R/2-r_e)})]\ . \tag{27}$$

We solve the two systems of Eqs. (24) and (26) and Eqs. (24) and (27) numerically. The results of the calculations for the model parameters are shown in Fig. 2(a)–2(c). In Fig. 2(a) we plot the dependence of the local frequencies ω_H and ω_O [Eqs. (24), (26), and (27)] versus absolute temperature T. The system of Eqs. (24) and (26) gives the curves corresponding to the roots $(\omega_H^{(0)},\omega_O^{(0)})$ as a function of temperature, while at the system of Eqs. (24) and (27) possesses two sets of roots: $(\omega_H^{(1)},\omega_O^{(1)})$ and $(\omega_H^{(2)},\omega_O^{(2)})$. The roots $(\omega_H^{(0)},\omega_O^{(0)})$ and $(\omega_H^{(2)},\omega_O^{(2)})$ correspond to the local minima $\tilde{\mathcal{F}}^{(0)}=\tilde{\mathcal{F}}(\omega_H^{(0)},\omega_O^{(0)})$ and $\tilde{\mathcal{F}}^{(2)}=\tilde{\mathcal{F}}(\omega_H^{(2)},\omega_O^{(2)})$ of the free energy $\tilde{\mathcal{F}}$ and the roots $(\omega_H^{(1)},\omega_O^{(1)})$ correspond to a local maximum $\tilde{\mathcal{F}}^{(1)}=\tilde{\mathcal{F}}(\omega_H^{(1)},\omega_O^{(1)})$ [Fig. 2(b)]. At temperatures higher than a critical temperature T_2 the system has only one minimum, $\tilde{\mathcal{F}}^{(0)}$, while at an even lower temperature there is a crossover to a single-well effective potential as the ground state. The dependence of the extremum values for the average proton displacement α_H versus T is shown in Fig. 2(c). One has to notice that the value of $\alpha_H^{(1)}$, corresponding to $\omega_H^{(1)}$, does not exist in the low-temperature region, where the argument of the hyperbolic inverse cosine [see Eq. (22)] is less than 1. This means that in that temperature region $[T<T_1\simeq 500$ K, where $\alpha_H^{(1)}(T)=0]$, the free energy presents a minimum, $\tilde{\mathcal{F}}^{(2)}$, corresponding to $\alpha_H^{(2)}$ and the frequencies $\omega_H^{(2)}$ and $\omega_O^{(2)}$, and a local maximum $\tilde{\mathcal{F}}^{(0)}$, corresponding to the frequencies $\omega_H^{(0)}$ and $\omega_O^{(0)}$ with $\alpha_H^{(0)}=0$.

At the temperature of $T_t\simeq 1650$ K $(T_1<T_t<T_2)$ the system undergoes a phase transition from the ground state with free energy $\tilde{\mathcal{F}}^{(2)}$ and proton location in left or right well, to the ground state with free energy $\tilde{\mathcal{F}}^{(0)}$, where the proton is situated between two oxygens $(\alpha_H^{(0)}=R/2)$. This phase transition corresponds to transition from ferro- to paraelectric phase in hydrogen-bonding ferroelectrics.[22]

B. Ionic defects

We studied ionic defects in a one-dimensional chain with $N=100$ cells, and used the Polak-Ribiere conjugate gradient method[40] to minimize the free energy of the system. The boundaries of the chain are held fixed: $\alpha_{O,1}=\alpha_{O,100}=0$, $\alpha_{H,1}=-\alpha_{H,100}=\pm\alpha_H^{(2)}$ [upper sign correspond to positive ionic defect (I^+), and lower sign corresponds to negative one (I^-)]. The minimization problem for $\tilde{\mathcal{F}}$, given by the Eqs. (5), (7), (9), and (10) with the boundary conditions mentioned above admits two kinds of stationary solutions. We define the stationary states of the defected chain for which the central proton $(n=51)$ is situated in the position $\alpha_{H,51}=0$ as the *centered states,*

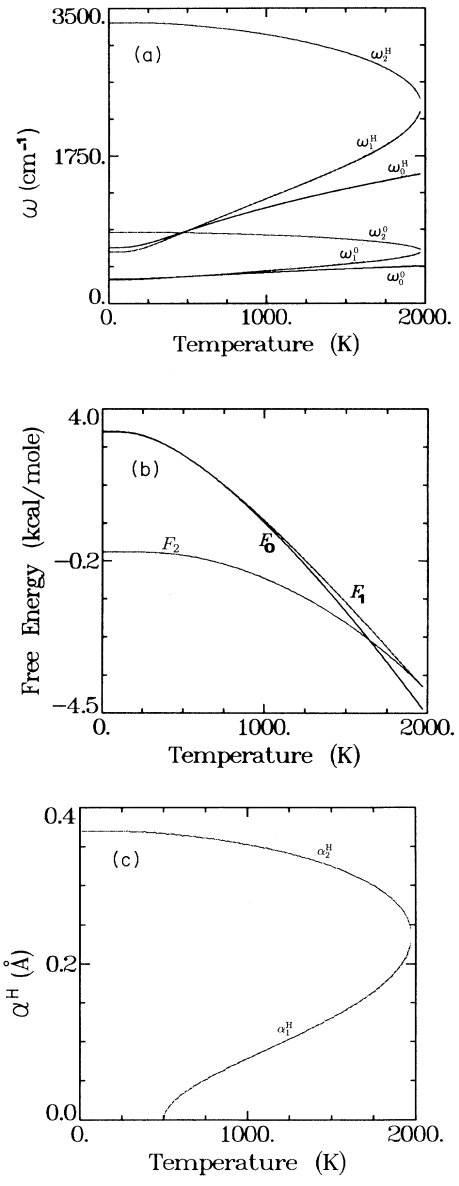

FIG. 2. Temperature dependence (a) of the roots ω_H and ω_O, (b) of the free energy, and (c) of the extremum values α_H.

and those for which two central protons occupy symmetrical positions ($\alpha_{H,50}=-\alpha_{H,51}$) as the *symmetrical states.* Two kinds of initial configurations of the system were chosen for each type of defect that correspond to the two possible stationary states, without, of course, imposing any symmetry. The first kind of initial conditions in the iteration procedure of the minimization problem, corresponding to the symmetrical stationary solution are $\alpha_{H,1}=\alpha_{H,2}=\cdots=\alpha_{H,50}=\pm\alpha_H^{(2)}$ and $\alpha_{H,51}=\alpha_{H,52}=\cdots=\alpha_{H,100}=\mp\alpha_H^{(2)}$. The second one corresponds to the centered stationary solution: $\alpha_{H,1}=\alpha_{H,2}=\cdots=\alpha_{H,50}=\pm\alpha_H^{(2)}$, $\alpha_{H,51}=0$, and $\alpha_{H,52}=\alpha_{H,53}=\cdots=\alpha_{H,100}=\mp\alpha_H^{(2)}$. The upper sign corresponds to the positive defect I^+ and the lower one to the negative I^-. The initial conditions for the other variational parameters $\alpha_{O,n}=0$, $\omega_{H,n}=\omega_H^{(2)}$, $\omega_{O,n}=\omega_O^{(2)}$, for all n, are used for both kinds of the stationary states of the defect.

As a result of the minimization procedure we have a solution which is the well-known kink or domain-wall solution. The temperature dependence of the free energy of the ionic kink defects is shown in Fig. 3 for both kind of stationary states. In all the cases the free energy shows a quite slow decrease in the physically interesting temperature interval (0–300 K). The formation energy for the I^+ defect is always higher than the I^- formation energy. The difference between the values of the free energy F for centered (I_{cent}) and symmetrical (I_{symm}) stationary states of the ionic defect is rather small comparatively with their absolute values. As one can see from Fig. 3, for low temperatures, $F^+_{symm}<F^+_{cent}$ and $F^-_{symm}<F^-_{cent}$ ($F^\pm_{symm}$ denotes free energy of the symmetrical stationary state of the positive and negative ionic defects and $F^\pm_{cent}$ denotes the same for the case of the centered defect). At $T\simeq 600$ K for the I^+ defect, the inequalities for I_{symm} and I_{cent} change sign. For the I^- defect this temperature is $T\sim 800$ K.

For a certain temperature of 250 K we show in Fig. 4 the shapes of the different kink solutions. The average displacement of the central chain atoms are shown for the hydrogen and the oxygen atoms. Away from the center, the oxygens approach their equilibrium position, while the hydrogens are situated in one of the two potential wells. Near the center, the atoms rearrange themselves to form the kink; the hydrogens climb the potential barrier, while the oxygens move now away from their equilibrium position. It is important to note that the negative defect oxygen atoms are displaced significantly, with respect to the hydrogens and also to the positive defect.

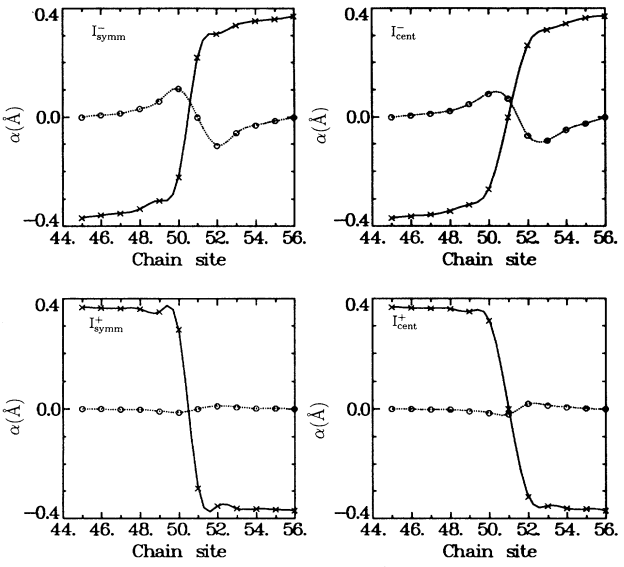

FIG. 4. Oxygen (○) and hydrogen (×) displacements for positive, negative, symmetric, and centered defects at $T=250$ K.

The Peierls-Nabbarro barrier as a function of temperature is shown in Fig. 5, for both the positive and negative defect. Due to the protonic repulsion, it is easier for a positive defect to move along the chain, once it has been created, than a negative one. This argument is true for a certain low-temperature region, while for higher temperatures the negative defect is favored. In order to investi-

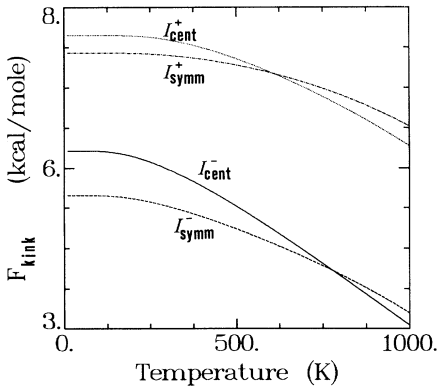

FIG. 3. Temperature dependence of the positive and negative ionic kink defect free energy for the symmetric and the centered type.

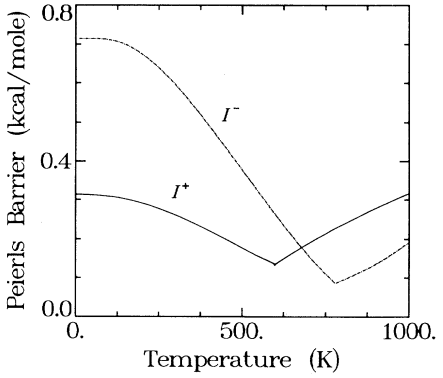

FIG. 5. The Peierls-Nabbarro barrier for the positive and negative defect as a function of temperature.

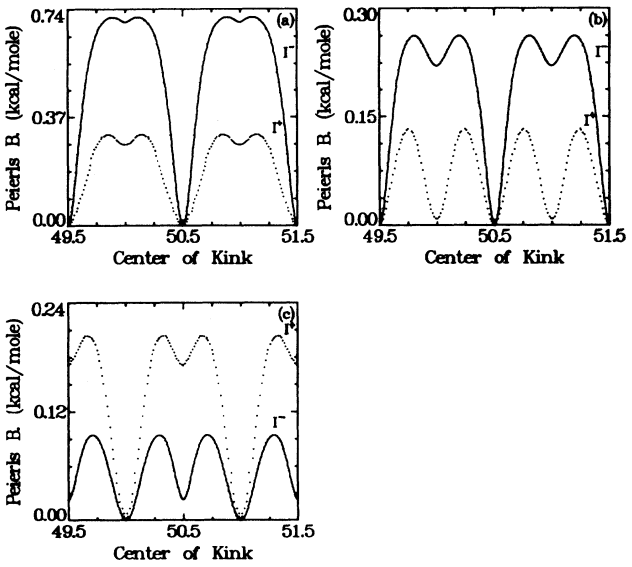

FIG. 6. The Peierls potential relief for (a) 10, (b) 600, and (c) 800 K.

gate the energy dependence of the position of the center of the defect, one constructs the Peierls potential relief of Fig. 6 for three different temperatures. For very low temperatures [Fig. 6(a)] it is evident that the positive defect has to overcome almost half of the barrier the negative defect has, in order to move from the state with a half-integer position of the center of the defect into the states with an integer position of the center. Also, both defects are stable in the centered state, since a minimum of the symmetrical state just starts to appear. As temperature rises [Fig. 6(b)] a minimum exists also for the symmetrical state for both types of defect, while for even higher temperatures [Fig. 6(c)], the negative defect becomes now easier to move, in accordance with Fig. 3(b).

VI. ANHARMONIC O-O INTERACTION

In the calculations of the previous section it is seen that the oxygen displacement is significant (see Fig. 4) especially for the symmetrical case. Thus it is important to take into consideration anharmonic terms in the O-O interaction. We introduce a Morse-type interaction also between the heavy ions. This means that the third term in Eq. (3) is replaced by the following:

$$U_{OO}=D_0[1-e^{-d_0(\rho_n-\rho_{n+1})}]^2 , \tag{28}$$

depending on the relative oxygen displacements. One proceeds with the variational method described in Sec. II, using the Hamiltonian terms given in Eqs. (1)–(4).

The two parameters D_0 and d_0 which characterize this potential are related to the energy of the hydrogen bond, $D_0=0.22$ eV (Ref. 27) and to the O-O vibrational force constant $d_0=(K_{OO}/2D_0)^{1/2}=2.28$ Å^{-1}.[37] The three DM parameters [Eq. (1)] are determined also in this case self-consistently, with a very similar algorithm as in the Appendix for the harmonic O-O interaction. Table III displays the set of parameters and force constants used in the numerical simulations.

The ground state (period 1 configuration) of the chain is found to have the same characteristics as the harmonic O-O potential, concerning the shape and the minima of the free energy as a function of temperature. There is only an increase in the temperature scale, of the order of 500 K, that translates to higher temperatures all the characteristic points of the curves. It is important to note here that the oxygen equilibrium distance is again held fixed, a rather artificial factor that would, if varied, reduce the temperature scales of the model to much more realistic figures.

Concerning the kink formation, as shown in Fig. 7(a), contrary to the harmonic O-O interaction, the free energy of the symmetrical kink configuration is lower than the centered one, for both the positive and negative kinks in all the interesting temperature range ($T<1000$ K). The fact that the Peierls-Nabbaro barrier [Fig. 7(b)] is higher for the negative I^- defect means[27] that the mobility of the positive I^+ defect is higher, in very good agreement with experiment.

The two Hamiltonians with the harmonic and anharmonic O-O interaction differ significantly only in the term that contains the ω_O. Other terms containing α_O are also negligible because they are related to the O-O

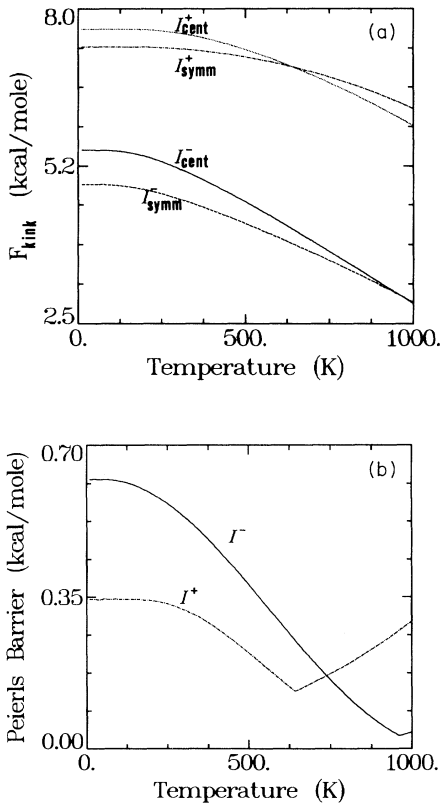

FIG. 7. (a) The kink free energy vs temperature for the anharmonic O-O interaction. (b) The Peierls-Nabbarro barrier vs temperature for the anharmonic O-O.

TABLE III. Set of parameters for the anharmonic O-O interaction.

D (kcal/mole)	d (Å^{-1})	r_e (Å)	R (Å)	k (N/m)	k_{HH} (N/m)	D_0 (kcal/mole)	d_0 (Å^{-1})
10.8	7.74	0.94	2.76	29.1	22.0	5.07	2.28

coupling constant k_{OO} which is chosen to be equivalent in both cases. On the other hand, ω is sensitive to the potential well shape and therefore has a different behavior.

VII. SUMMARY

This model contributes two important points to the study of hydrogen-bonded chains. First, it simulates the hydrogen bond in a realistic way. This is accomplished by the double Morse potential, which has the advantage to describe the protonic motion for various O-O distances with the same potential parameters.[38] Second, this model is for a variable ($T\neq 0$) temperature and includes zero-point energy effects and entropic contributions, which are very important for the light mass protons, and the effect on the proton barrier due to the heavy sublattice motion. The study of the ground state of the chain, which is the period 1 structure, reveals that for low temperatures, the free energy has two symmetrical global minima, with one local maximum in between. As temperature rises, the central local maximum transforms to a local minimum and two other local maxima are created symmetrically. At the phase transition temperature the central local minimum becomes the global one and the ground state is now the paraphase, which means that the average proton position is in the middle point between two oxygens.

The two kinds of stationary defects (positive and negative), in their symmetrical and centered configurations, which can exist on the chain, are both stable for the chain. In the physically interesting temperature region of 0–300 K, the energy of the positive defect is always higher than the negative ones and the symmetrical state has a lower energy than the centered one, for both the harmonic and anharmonic O-O interactions. This fact is related to the changes in the barrier of the effective proton potential, due to the heavy sublattice motion. Of course, there are also important entropic contributions.

It should be remarked that it is not surprising that the centered configuration is stable. In this case the central atom sits in a local minimum of the free energy hypersurface, unlike the classical case, where the particle sits on a maximum of the potential energy. This is similar to the case of the Kapitza inverted pendulum,[41] which is stabilized under fast fluctuating forces. It is the entropic effect that lowers the free energy, since the available phase space in this case includes both wells. This situation can exist even at $T=0$ due to the zero-point energy, which includes quantum fluctuations. Depending on the form of the O-H potential, the effect can vary. In fact, the $\alpha=0$ can also become a global minimum.

With this model we demonstrate the importance of zero-point energy. In fact, the effect of the zero-point energy and thermal fluctuations is to lower the energy of the ionic defects significantly. This lowering is much more important than that which is produced by a significant change of the interaction parameters and it is also important at higher temperatures. The parameter values are chosen for the particular case of ice. Nevertheless, the exact numerical results have only a qualitative value and, in fact, are not trustworthy much higher than 300 K. This is related with the limited validity of all the parameters used, over a range of temperatures. Outside this temperature region, there are significant charge redistributions compounded by dynamical effects due to the light proton that cannot be taken into account in this simple model.

It is important to note that the increased mobility (low Peierls barrier) found within this model, i.e., the energy required to move a defect once it is created, is due to the thermal fluctuations and the zero-point energy. A classical model with the same parameters[27] has found a higher effective Peierls barrier.

Significant effects will come from the dependence of the O-H stretching vibration due to the O-O vibration amplitude.[42] The inclusion of anharmonic O-O interaction does not change significantly the displacements of protons and heavy ions but influences a lot the local frequencies, which are important for the determination of the free energy. On top of this the anharmonicity of the O-O vibration will act on the O-H vibration as discussed in the previous section.

ACKNOWLEDGMENTS

Part of this work was supported by European Economic Community Science Project No. SCI-0229-C. The authors benefited from extensive discussions with Y. Gaididei, Y. Kivshar, A. Savin, and A. Zolotariuk. One of us (O.Y.) would like to express his thanks for the hospitality of the University of Crete and the Research Center of Crete.

APPENDIX

Taking into account the ground-state conditions (13) the expression (10) for the DM part of the ground-state free energy $\tilde{\mathcal{F}}$ takes the form

$$\begin{aligned}\langle U_{OH}\rangle = D(2 &- 2e^{d^2f/4-d(R/2+\alpha_H-r_e)} \\ &+ e^{d^2f-2d(R/2+\alpha_H-r_e)} \\ &- 2e^{d^2f/4-d(R/2-\alpha_H-r_e)} \\ &+ e^{d^2f-2d(R/2-\alpha_H-r_e)}),\end{aligned} \tag{A1}$$

where f is expressed by Eq. (23). It is important to emphasize that the solutions $(\omega_H^{(0)},\omega_O^{(0)})$ of the system of Eqs. (24) and (26), corresponding to the case $\alpha_H=0$, can give a local maximum or local minimum of the free energy $\tilde{\mathcal{F}}$, depending on the distance R between the heavy ions. If

the distance R is large enough the potential (A1) has two minima $\alpha_{H,1,2}$ [Eq. (22)] that gives us an expression for the equilibrium OH-bond length:

$$r_0=\frac{R}{2}-\frac{1}{d}\operatorname{arcosh}\left\{\frac{1}{2}\exp\left[-\frac{3}{4}d^2f+d\left[\frac{R}{2}-r_e\right]\right]\right\} \tag{A2}$$

and a maximum at $\alpha_H=0$. When we decrease R, at some distance this maximum transforms into local minimum of the energy $\tilde{\mathcal{F}}$. At critical distance $R=R_{cr}$ this local minimum will become the global minimum of the free energy $\tilde{\mathcal{F}}$, i.e., $\tilde{\mathcal{F}}|_{\alpha_H=0}<\tilde{\mathcal{F}}|_{\alpha_H=\alpha_{H,1}}$, when $R<R_{cr}$.

Using Eq. (27), one can write the following expression for the stretching force constant k_{OH}

$$k_{OH}=\left.\frac{\partial^2\tilde{\mathcal{F}}}{\partial\alpha_H^2}\right|_{\alpha_H=\alpha_{H,1,2}}=2k_{HH}+2Dd^2(-e^{-d^2f/2}+4e^{d^2f-2d(R/2-r_e)}) . \tag{A3}$$

From (A2) and (A3) we have the formulas for parameters r_e and D:

$$r_e=\frac{R}{2}-\frac{3}{4}df-\frac{1}{d}\ln\left\{2\cosh\left[d\left[\frac{R}{2}-r_0\right]\right]\right\}, \tag{A4}$$

$$D=\frac{1}{2d^2}(k_{OH}-2k_{HH})e^{d^2f/2}\operatorname{cotanh}^2\left[d\left[\frac{R}{2}-r_0\right]\right] . \tag{A5}$$

Finally, the algorithm to define the parameters d, r_e, and D is the following. We fix the distance $R=R_{cr}$ and change the parameter d. For each value of d, using Eqs. (A4) and (A5) we define parameters r_e and D and calculate the values of the energy $\tilde{\mathcal{F}}$ at the distances $\alpha_H=0$ and $\alpha_H=\alpha_{H,1}$. When these two values are equal we have the parameter d that needs to be found. This algorithm can be easily realized numerically.

*Permanent address: Bogolyubov Institute for Theoretical Physics, Kiev, 252143, Ukraine.

[1]A. Kuwada, A. R. McGhie, and M. M. Labels, J. Chem. Phys. **52**, 1438 (1970).
[2]D. M. Alexander and J. A. Krumhansl, Phys. Rev. B **33**, 7172 (1986).
[3]R. W. Jansen, R. Bertoncini, D. A. Pinuick, A. I. Katz, R. C. Hanson, O. F. Sankey, and M. O'Keeffe, Phys. Rev. B **35**, 9830 (1987); M. Springborg, *ibid.* **38**, 1438 (1988).
[4]I. D. Brown, Acta Crystallogr. **17**, 654 (1964); V. H. Schmidt, J. E. Drumheller, and F. L. Howell, Phys. Rev. B **4**, 4582 (1971).
[5]J. F. Nagle and H. J. Morowitz, Proc. Natl. Acad. Sci. **75**, 298 (1978); J. F. Nagle, M. Mille, and H. J. Morowitz, J. Chem. Phys. **72**, 3959 (1980).
[6]J. Vanderkoy, J. D. Cuthbert, and H. E. Petch, Can. J. Phys. **42**, 1871 (1964).
[7]Ph. Colomban and A. Novak, J. Mol. Struct. **177**, 277 (1988).
[8]J. D. Bernal and R. H. Fowler, J. Chem. Phys. **1**, 515 (1933).
[9]D. Oesterhelt and W. Stoeckenius, Proc. Natl. Acad. Sci. **70**, 2853 (1973); H. Merz and G. Zundel, Biochem. Biophys. Res. Commun. **101**, 540 (1981).
[10]B. Bullmer, E. Engelhart, and N. Riehl, in *Physics of Ice,* edited by N. Riehl, B. Bullmer, and E. Engelhart (Plenum, New York, 1969), p. 416.
[11]L. Onsager and L. K. Runnels, J. Chem. Phys. **10**, 1089 (1969).
[12]C. Jackard, Helv. Phys. Acta **32**, 89 (1959).
[13]P. R. Camp, W. Kiszenick, D. Arnold, Helv. Phys. Acta **32**, 450 (1959).
[14]J. F. Nagle, in *Proton Transfer in Hydrogen-Bonded Systems,* edited by T. Bountis (Plenum, New York, 1992), p. 17.
[15]A. V. Zolotariuk, St. Pnevmatikos, and A. V. Savin, Physica D **44**, (1991).
[16]M. Peyrard, S. Pnevmatikos, and N. Flytzanis, Phys. Rev. A **36**, 903 (1987).
[17]A. V. Zolotaryuk, in *Biophysical Aspects of Cancer,* edited by J. Fiala and J. Pokorný (Chalres University, Prague, 1987), p. 179.
[18]St. Pnevmatikos, Phys. Rev. Lett. **60**, 1534 (1988).
[19]J. H. Weiner and A. Askar, Nature (London) **226**, 842 (1970).
[20]N. Flytzanis, S. Crowley, and V. Celli, Phys. Rev. Lett. **39**, 891 (1977).
[21]T. R. Koehler, in *International School of Physics Enrico Fermi,* edited by S. Califano (Academic, New York, 1975), Vol. LV.
[22]S. Tanaka, Phys. Rev. B **42**, 10488 (1990).
[23]V. Ya. Antonchenko, A. S. Davydov, and A. V. Zolotariuk, Phys. Status Solidi B **115**, 631 (1983).
[24]P. T. Dinda and E. Coquet, J. Phys. Condens. Matter **2**, 6953 (1990).
[25]Y. Kashimori, T. Kikushi, and K. Nishimoto, J. Chem. Phys. **77**, 1904 (1982).
[26]E. S. Kryachenko, Chem. Phys. **143**, 359 (1990).
[27]A. V. Savin and A. V. Zolotaryuk, Phys. Rev. A **44**, 8167 (1991).
[28]R. P. Feynman and A. R. Hibbs, *Quantum Mechanics and Path Integrals* (McGraw-Hill, New York, 1965).
[29]G. Vlastou-Tsinganos, N. Flytzanis, and H. Büttner, J. Phys. A **23**, 4533 (1990).
[30]S. Shimamura, S. N. Khanna, and P. Jena, Phys. Rev. B **40**, 2459 (1989).
[31]S. Kirkpatrick, C. D. Gellatt, and M. P. Vechi, Science **220**, 671 (1983).
[32]G. Vlastou-Tsinganos, N. Flytzanis, and H. Büttner, J. Phys. A **23**, 225 (1990).
[33]O. Yanovitskii, N. Flytzanis, and G. Vlastou-Tsinganos, in *Proton Transfer in Hydrogen-Bonded Systems,* edited by T. Bountis (Plenum, New York, 1992), p. 351.
[34]St. Pnevmatikos, A. V. Savin, A. V. Zolotaryuk, Yu. S. Kivshar, and M. J. Velgakis, Phys. Rev. A **43**, 5518 (1991).
[35]E. Matsushita and T. Matsubara, Progr. Theor. Phys. **67**, 1 (1982).
[36]P. V. Hobbs, *Ice Physics* (Clarendon, Oxford, 1974).
[37]P. Bosi, R. Tubino, and G. Zerbi, in *Physics and Chemistry of Ice,* edited by E. Whalley, S. J. Jones, and L. W. Gold (Royal

Society of Canada, Ottawa, 1973).
[38]X. Duan and S. Scheiner, J. Mol. Struct. **270**, 173 (1992).
[39]K. Luth and S. Scheiner, Intern. J. Quantum Chem. Symp. No. **26**, 817 (1992).
[40]W. Press, B. P. Flannery, S. A. Teukovsky, and W. T. Vetterling, *Numerical Recipes* (Cambridge University Press, Cambridge, 1986).
[41]L. D. Landau and E. M. Lifshitz, *Mechanics* (Pergamon, New York, 1976).
[42]E. R. Lippincott and R. Schroeder, J. Chem. Phys. **23**, 1099 (1955).